

## Rituximab-Mediated Cell Signaling and Chemo/Immuno-sensitization of Drug-Resistant B-NHL Is Independent of Its Fc Functions

Mario I. Vega,<sup>1,2</sup> Sara Huerta-Yepez,<sup>1,2</sup> Melisa Martinez-Paniagua,<sup>2</sup> Bernardo Martinez-Miguel,<sup>2</sup> Rogelio Hernandez-Pando,<sup>3</sup> Cesar R. González-Bonilla,<sup>2</sup> Paul Chinn,<sup>4</sup> Nabil Hanna,<sup>4</sup> Kandasamy Hariharan,<sup>4</sup> Ali R. Jazirehi,<sup>1</sup> and Benjamin Bonavida<sup>1</sup>

**Abstract Purpose:** Rituximab [chimeric anti-CD20 monoclonal antibody], alone or combined with chemotherapy, is used in the treatment of non-Hodgkin's lymphoma (NHL). Rituximab binds to CD20 and inhibits intracellular survival/growth pathways leading to chemo/immunosensitization of tumor cells *in vitro*. The contribution of rituximab Fc-FcR interaction in signaling is not known. This study examined the role of Fc-FcR interactions in rituximab-induced signaling using rituximab (Fab')<sub>2</sub> fragments as well as rituximab devoid of the CH2 Fc-binding domain (CH2').

**Experimental Design:** Rituximab (CH2') and rituximab (Fab')<sub>2</sub> were tested for their activity on B-NHL cell lines. Cell signaling and sensitization to chemotherapy and immunotherapy were examined. The *in vitro* studies were validated in mice bearing tumor xenografts.

**Results:** Although the modified antibodies were defective in antibody-dependent cellular cytotoxicity and complement-dependent cytotoxicity functions, they retained all other biological activities such as inhibition of cell proliferation, induction of cell aggregation, and apoptosis induction. In addition, similar to rituximab, the modified antibodies inhibited the activity of cell survival/growth pathways and their associated transcription factors (e.g., NF- $\kappa$ B, YY1, SP-1), and signal transducers and activators of transcription 3 (STAT-3), and downregulated the expression of antiapoptotic gene products, such as Bcl-2/Bcl<sub>xL</sub>, which regulate drug resistance. The modified antibodies, similar to rituximab, sensitized resistant B-NHL cells to both CDDP and Fas ligand-induced apoptosis. Furthermore, treatment of nude mice bearing Raji tumor cell xenografts with the combination of rituximab (Fab')<sub>2</sub> or rituximab and CDDP resulted in similar and significant inhibition of tumor growth.

**Conclusion:** These findings reveal that rituximab-mediated inhibition of intracellular signaling pathways and leading to chemo/immuno-sensitization of resistant B-NHL is Fc independent. (Clin Cancer Res 2009;15(21):6582-94)

Rituximab (chimeric mouse anti-human CD20 monoclonal antibody) is a genetically engineered monoclonal antibody used for the treatment of patients with relapsed or refractory low-grade or follicular B-cell non-Hodgkin's lymphoma (NHL) and in patients with relapsed stage III/IV follicular lymphoma (1, 2). Rituximab is composed of murine Variable (V) and human IgG1 Constant (C) regions. Rituximab functions by binding to the CD20 antigen expressed on the surface of normal and malignant B cells. The overall response in patients is 50% when it is used as a single agent (3), and the response rate

phoma (1, 2). Rituximab is composed of murine Variable (V) and human IgG1 Constant (C) regions. Rituximab functions by binding to the CD20 antigen expressed on the surface of normal and malignant B cells. The overall response in patients is 50% when it is used as a single agent (3), and the response rate

**Authors' Affiliations:** <sup>1</sup>Department of Microbiology, Immunology, and Molecular Genetics, Jonsson Comprehensive Cancer, David Geffen School of Medicine, University of California, Los Angeles, California; <sup>2</sup>Unidad de Investigación Médica en Inmunología e Infectología, Hospital de Infectología, CMN "La Raza," IMSS, México City, México; <sup>3</sup>Sección de Patología Experimental, Departamento de Patología, Instituto Nacional de Ciencias Médicas y Nutrición Salvador Zubirán, México City, México; <sup>4</sup>Biogen-Idec, Inc., San Diego, California.

Received 5/19/09; revised 7/21/09; accepted 8/3/09; published OnlineFirst 10/27/09.

**Grant support:** Jonsson Comprehensive Cancer Center (A.R. Jazirehi and M.I. Vega), the University of California at Los Angeles AIDS Institute (M.I.

Vega) and Fogarty International Center Fellowship grant D43 TW00013-14 (M.I. Vega), and the UC-MEXUS-CONACYT (S.H. Yepez).

The costs of publication of this article were defrayed in part by the payment of page charges. This article must therefore be hereby marked *advertisement* in accordance with 18 U.S.C. Section 1734 solely to indicate this fact.

**Note:** Supplementary data for this article are available at Clinical Cancer Research Online (<http://clincancerres.aacrjournals.org/>).

**Requests for reprints:** Benjamin Bonavida, Department of Microbiology, Immunology and Molecular Genetics, University of California, 10833 Le Conte Avenue A2-060 CHS, Los Angeles, CA 90095-1747. Phone: 310-825-2233; Fax: 310-206-2791; E-mail: [bbonavida@mednet.ucla.edu](mailto:bbonavida@mednet.ucla.edu).

© 2009 American Association for Cancer Research.  
doi:10.1158/1078-0432.CCR-09-1234

## Translational Relevance

Rituximab has been used for the treatment of CD20-expressing B-cell malignancies. The *in vivo* mechanism of action has been proposed to be through antibody-dependent cellular cytotoxicity, complement-dependent cytotoxicity, and apoptosis. A subset of patients exhibits a poor clinical response due to Fc polymorphism. Reported studies showed that rituximab mediates cell signaling and inhibits several survival pathways, and sensitizes resistant tumors to apoptosis by chemotherapeutic drugs. In addition, the combination of rituximab and chemotherapy results in a significant clinical response. The role of the Fc fragment of rituximab in mediating cell signaling and chemosensitization was examined and was found to be Fc independent. These studies suggest that the chemosensitizing effect of rituximab should also occur in patients with Fc polymorphism.

is significantly higher when rituximab is used in combination with chemotherapy (4). The antitumor effect of rituximab depends, in part, on FcγR-dependent immune activation (5). Also, it has been reported that human FcγR polymorphism correlates with the efficacy of B-tumor cell depletion and clinical response (6, 7). It has been shown that rituximab can induce apoptosis in some systems but not others (8, 9). In addition to the above mechanisms, we have reported that rituximab can also sensitize resistant tumor cells to apoptosis by chemotherapeutic drugs and Fas ligand. Sensitization was the result of rituximab-mediated inhibition of cell survival signaling pathways and downregulation of antiapoptotic resistant factors (10–13).

Modulation of the signaling pathways upon treatment of B-NHL cells with rituximab might be the direct result of triggering the CD20 receptor by rituximab (Supplementary Fig. S1) or, conceivably, through cross-linking of the Fc fragment of rituximab with FcRs expressed on the tumor cells or on host-effector cells. Cross-linking of Fc on target cells by rituximab may either activate or inhibit intracellular signaling pathways and the balance can lead to the observed rituximab-mediated inhibition of survival pathways. Four classes of Fc receptors have been identified, namely, FcγRI, FcγRII, FcγRIII, and FcγRIV. The activating and inhibitory receptors (FcγRIIB) transmit their signal via immune receptor tyrosine-based activation motif and inhibitory immune receptor tyrosine-based inhibitory motif (ITIM), respectively (14, 15). The FcR receptors show significant differences in their affinity for individual Fc isotypes (16, 17). Thus, it is conceivable to postulate that rituximab-mediated cell signaling may be dependent, in part, on the rituximab Fc fragments triggering FcR-bearing cells.

To address the role of Fc-FcR interactions in rituximab-mediated cell signaling and sensitization *in vitro*, we have prepared (Fab')<sub>2</sub> fragments from rituximab and have genetically constructed rituximab molecules devoid of the CH2 domain that is responsible for both antibody-dependent cellular cytotoxicity (ADCC) and complement-dependent cytotoxicity (CDC) effector functions (18, 19). In the preparation of monomeric CH2-deleted antibodies, a dimeric form was also gener-

ated following strong noncovalent interactions. The present study investigated the functional role of the Fc fragment of rituximab in cell signaling and chemo/immunosensitization. By comparison with rituximab, the following objectives were investigated using B-NHL cell lines as models: (a) Do the modified antibodies [rituximab (Fab')<sub>2</sub> and rituximab (CH2')] inhibit tumor cell proliferation and require cross-linking with a secondary anti-Ig antibody for the induction of apoptosis? (b) Do the modified antibodies trigger the cells and inhibit the activity of the constitutively activated p38 mitogen-activated protein kinase (MAPK) cell survival pathway (and associated transcription factors) and, consequently, inhibition of the expression of the antiapoptotic gene products Bcl-2/Bcl-x<sub>L</sub> that regulate resistance? (c) Do the modified antibodies sensitize resistant B-NHL cell lines to apoptosis induced by chemotherapeutic drugs and Fas ligand? and (d) Does rituximab (Fab')<sub>2</sub> mimic rituximab in the inhibition of tumor growth xenograft when used in combination with CDDP? The findings show the Fc independence of rituximab-mediated biological effects.

## Materials and Methods

### Cell lines

The Ramos, Raji, and Daudi cell lines were purchased from American Type Culture Collection. The AIDS-NHL B-cell line 2F7 was kindly provided by Dr. Otoniel Martinez-Maza (Jonsson Comprehensive Cancer Center, Los Angeles, CA; ref. 10). Cells were grown in RPMI 1640 (Mediatech, Cellgro) supplemented with 10% heat-inactivated fetal bovine serum (Life Technologies, Invitrogen Co.) and 1% bacteriostatic solution containing 10,000 U/mL penicillin G, 10 mg/mL streptomycin, and 25 μg/mL fungizone (Cellgro). Cells were cultured in 5% CO<sub>2</sub> at 37°C.

### Antibodies and reagents

Rituximab was commercially obtained. The genetically engineered rituximab with deleted CH2 domain (monomeric and dimeric CH2') was developed at Biogen-IDEC, Inc. Human IgG (Sigma) antibody was used as control. The entire light chain, heavy variable, CH1 and CH3 domains were not changed. In addition, the first residue of the hinge region was changed from alanine to valine. The expression construct was transfected into Chinese hamster ovary DG44 cells secreting a mixture of antibodies differentiated by disulfide formation in the hinge region. One form has properly formed disulfide and is the "Monomeric" antibody, rituximab (CH2'). The second form has intrachain disulfides enabling noncovalent interactions between two antibodies to form a "Dimeric" antibody, rituximab (CH2') Dimer. This Dimer antibody is extremely stable as evidenced by the fact that SDS is required to break the interaction. The Monomeric and Dimeric forms were separated by high performance liquid chromatography. The rituximab (Fab')<sub>2</sub> fragment was also obtained from Biogen-IDEC. It was prepared by pepsin digestion and purified to homogeneity as determined by SDS-PAGE analysis (Supplementary Fig. S2). The anti-Fas and anti-Bcl-2 antibodies used for Western were purchased from Dako, the agonist antibody against Fas (CH-11) and anti-Fas antibody (UB2) used for flow were purchased from MBL. The anti-phospho Lyn, anti-Lyn, anti-p38 MAPK antibodies, and anti-Bcl-x<sub>L</sub> antibody were purchased from Cell Signaling and Santa Cruz, respectively.

### Antibody-dependent cellular cytotoxicity

Raji cells (CCL-86, American Type Culture Collection) were grown in RPMI 1640 (Irvine Scientific) supplemented with 10% heat-inactivated fetal bovine serum (Hyclone), 2 mmol/L L-glutamine, 100 units/mL of penicillin, and 100 μg/mL of streptomycin. Activated human peripheral blood mononuclear cells (PBMC) were used as effector cells and

<sup>51</sup>Cr-labeled Raji as target. PBMC were isolated from whole blood of healthy donors using Histopaque (Sigma-Aldrich Corp.) and were cultured at a concentration of  $5 \times 10^6$  cells/mL in complete medium with 20 U/mL recombinant human interleukin 2 (Invitrogen) in 75-cm<sup>2</sup> tissue culture flasks at 37°C and 5% CO<sub>2</sub>. After overnight culture, 10<sup>6</sup> Raji target cells were labeled with 150 μCi of <sup>51</sup>Cr (Amersham Pharmacia Biotech) for 1 h at 37°C and 5% CO<sub>2</sub>. The cells were washed four times and resuspended in 5 mL of complete medium; 50 μL of cell suspension was dispensed into each well containing equal volume of test or control antibodies. All wells were plated in triplicate into a 96-well, round-bottomed tissue culture plate. The effector cells were harvested, washed once with complete medium, and added at  $1 \times 10^6$  cells in 100 μL volume per well to obtain a 50:1 effector to target ratio. The following control wells were also included in triplicate: target cells incubated with 100 μL complete medium to determine spontaneous release and target cells incubated with 100 μL 0.5% Triton X-100 (Sigma-Aldrich Corp.) to determine maximum release. The culture was incubated for 4 h at 37°C and 5% CO<sub>2</sub>, and the <sup>51</sup>Cr released in the culture supernatant due to cell lysis was determined on a γ counter (ISODATA). The cytotoxicity was expressed as the percentage of specific lysis and calculated as follows:

$$\% \text{Specific lysis} = \frac{{}^{51}\text{Cr release of test samples} - \text{spontaneous } {}^{51}\text{Cr release}}{\text{Maximum } {}^{51}\text{Cr release} - \text{spontaneous } {}^{51}\text{Cr release}} \times 100$$

#### Complement-dependent cytotoxicity

The CDC activity of antibodies was determined using B-cell lines and rabbit complement. Dilutions of antibodies were made and 50 μL were dispensed into each 96-well plates in triplicates. The Raji cells were labeled with <sup>51</sup>Cr (150 μCi/10<sup>6</sup> cells) for 1 h at 37°C and 5% CO<sub>2</sub>. The cells were washed four times and resuspended in complete medium, and  $1 \times 10^4$  cells in 50 μL were dispensed into each well. Normal rabbit complement (100 μL; ICN/Cappel Pharmaceuticals, Inc.) diluted 1:5 in complete medium was added. Materials and Methods for the spontaneous and maximum release control and set up were calculated as described above for ADCC. The cultures were incubated 4 h at 37°C and 5% CO<sub>2</sub>. The radioactivity released into the culture supernatant was determined on a γ counter. The formula for calculating the percentage of specific cell lysis is described above in ADCC. Also, CDC was achieved with human serum as source of complement and cytotoxicity assessed by flow as described (10).

#### Isolation of natural killer cells from human PBMCs and cytotoxic assays

PBMC were isolated from healthy donors by Lymphoprep (Axis-Shield PoC) gradient centrifugation. The subpopulations of natural killer (NK) cells were purified from isolated PBMC using negative selection and Dynabeads (Dyna, Invitrogen) according to the manufacturer's instructions. The purity, checked by flow cytometry (CD56<sup>+</sup>, CD16<sup>+</sup>), was >95% (data not shown). The purified NK cells were used as effectors cells for the cytotoxic assays described below.

Cell-mediated cytotoxicity was measured by CytoTox 96 Non-Radioactive Cytotoxicity Assay (Promega Co.) based on assessment of the total release of cytoplasmic lactate dehydrogenase into the cultured medium as a consequence of damaged cell membranes. Raji cells were incubated in 5% CO<sub>2</sub> at 37°C for 18 h in the absence or presence of IgG control, rituximab, or (Fab')<sub>2</sub> rituximab. Raji cells were mixed with the effectors cells at the effector to target ratio of 40:1 and incubated at 37°C for 6 h in the presence or absence of CDDP (5 μg/mL). The assay was done according to the manufacturer's instructions. The specific lysis was calculated by a standard formula according to the manufacturer's instructions.

#### Flow cytometric assays

**Fas expression.** An anti-human IgG-FITC antibody (Immunotech, Beckman Coulter Co.) was used to determine the cell binding of the

various rituximab antibodies. Cells were suspended at 10<sup>6</sup>/mL in medium and were treated with an optimal concentration (137 nmol/L) antibody for 60 min, washed twice with PBS, and incubated with 3 μL of anti-IgG human-FITC. Immunofluorescence was carried out as described (11, 12). Extracellular detection was determined in cells treated with anti-Fas antibody or isotype control. The cells were washed twice and incubated with anti-mouse antibody phycoerythrin conjugated (Pharmin-gen) and analyzed by flow cytometry with a FACS Epics-XL MCL flow cytometer (Coulter, Inc.).

**Active caspase-3.** Active caspase-3 was analyzed by flow cytometry using an FITC-conjugated anti-active caspase-3 monoclonal antibody (BD Pharmingen) as was described previously (11, 12). Briefly,  $2 \times 10^6$  cells per sample were preincubated with rituximab (137 nmol/L) for 26 h and CH-11 antibody was added for an additional 18 h. For cross-linking, the cells were incubated with rituximab (137 nmol/L) and anti-human IgG antibody (342 nmol/L; ICN Pharmaceuticals) for 24 h. The cells were stained intracellularly with anti-active caspase 3 antibody and the samples were analyzed by flow cytometry. Population data were acquired on a Flow centre EPICS<sup>R</sup> XL-MCL (Coulter, Co.) with the System II Software and the percent-positive cells were recorded.

#### Microscopic analysis

2F7 (10<sup>6</sup>) cells were grown in six-well plates and treated with different antibodies [rituximab, rituximab (Fab')<sub>2</sub>, rituximab (CH<sub>2</sub>)<sub>2</sub>, rituximab (CH<sub>2</sub>)<sub>2</sub> Dimer] at 137 nmol/L for 6 h. The cells were visualized on an inverted microscope. Images were captured using Adobe Photoshop 3.0.5 (Adobe System, Inc.) and a Sony DKC-5000 digital camera.

#### Measurement of cell growth

2F7 cells ( $2 \times 10^5$ /mL) were incubated at 37°C for different time periods in the presence and absence of different concentrations of various rituximab antibodies (6, 9, 68.5, 137, and 274 nmol/L). The irrelevant human IgG isotype antibody (342 nmol/L) was used as control. Cells were stained with trypan blue and viable cells were counted using light microscopy.

#### Western blot analysis for protein expression

This was done as described previously (10). 2F7 and Ramos cells were incubated at 37°C for 24 h. Cells extracts for protein analysis were prepared by lysing  $2 \times 10^6$  cells on ice with cold 200 μL of radioimmunoprecipitation assay buffer [1% NP40, 0.1% SDS, 0.5% deoxycholic acid, complete protease inhibitor cocktail tablets (Roche Diagnostic Co.), and 1× PBS]. Lysates were transferred to microcentrifuge tubes and sonicated in SONICATOR, model W-220F (Heat-System Ultrasonic, Inc.), for 10 s. Lysates were centrifuged at 12,000 × g at 4°C for 5 min. Protein concentration was quantified using the Bio-Rad protein assay (Bio-Rad Laboratories). Gel loading buffer Bio-Rad (Bio-Rad Laboratories) was added to the cell lysates, at a 1:1 volume. Samples were boiled for 5 min and were separated on 12% SDS-polyacrylamide minigels and transferred to nitrocellulose membrane Hybond enhanced chemiluminescence (Amersham Pharmacia Biotech) in Trans-Blot SD semidry Transfer cell System (Bio-Rad).

#### Gel mobility shift assays

This was done as described (10). Briefly, cells (10<sup>6</sup>) were harvested after treatment and washed twice with cold Dulbecco PBS (Cellgro). After washing, the cells were lysed in 1 mL of NP40 lysis buffer [10 mmol/L Tris-HCl (pH 7.5), 10 mmol/L NaCl, 3 mmol/L MgCl<sub>2</sub>, and 0.5% NP40] on ice for 5 min. Samples were centrifuged at 300 × g at 4°C for 5 min. The pellet was washed twice in NP40 buffer. Nuclei were then lysed in nuclear extraction buffer [20 mmol/L HEPES (pH 7.9), 25% glycerol, 0.42 mmol/L NaCl, 1.5 mmol/L MgCl<sub>2</sub>, 0.2 mmol/L EDTA, 0.5 mmol/L phenylmethylsulfonyl fluoride, and 0.5 mmol/L DTT] and sonicated 10 s at 4°C. The protein concentration was determined using the Bio-Rad protein assay. The nuclear proteins were frozen at -80°C. Both buffers contained the complete protease inhibitor

cocktail tablets from Roche. Nuclear protein (5 µg) was mixed for 30 min at room temperature with Biotin-labeled oligonucleotide probe NF-κB, Sp1, YY1, and signal transducers and activators of transcription 3 (STAT-3), using the electrophoretic mobility shift assay kit purchased from Panomics, Inc., following the manufacturer's instructions. Ten microliters was subjected to 5% PAGE for 90 min in Tris-borate EDTA buffer (Bio-Rad Laboratories), and transferred to Nylon transfer membrane Hybond-N+ (Amersham) using the Trans-Blot SD semidry Transfer cell System (Bio-Rad). The membranes were transferred to a UV Cross-linker FB-UVXL-1000 Fisher technology (Fisher Scientific) for 3 min. The detection was made as per the manufacturer's instructions, after the membranes were exposed using Hyperfilm enhanced chemiluminescence (Amersham Pharmacia Biotech).

#### ***In vivo* inhibition of Raji tumor xenograft in nude mice**

The Raji ascites model was adapted from Zhu et al. (20) and Xiong et al. (21). Briefly, Raji cells ( $6.5 \times 10^6$ ) were inoculated i.p. into 6- to 8-wk-old female athymic Nude-FoxN (Hardan). All mice were primed i.p. with 200 µL of pristane (Sigma) to induce inflammation on the week before cell inoculation. Treatment started 1 wk after tumor cell inoculation by i.p. injection of rituximab or (Fab')<sub>2</sub> rituximab (100 µg/200 µL; five animals per group). One and 2 d after antibody treatment, CDDP (4 mg/Kg in 200 µL) was administered (i.p.) for two cycles of 10-d intervals. At 60 d after tumor inoculation, the animals were sacrificed, and various organs were recovered for histologic and pathologic analyses. Organs were analyzed by immunohistologic staining with a series of antibodies to confirm human tumor cells of B-cell origin. The animal experiments were done in accordance with allowed institutional and international regulations, and research protocols were approved by them.

**Spleen histology and morphometric analysis.** After sacrifice, the spleens were removed from the mice. Spleen tissues were fixed with 4% (v/v) neutral buffered formalin. The specimens were dehydrated and embedded in paraffin. For histologic examination, 4-µm sections of fixed embedded tissues were cut on a Leica model 2165 rotary microtome (Leica), placed on glass slides, deparaffinized, and stained sequentially with H&E to assess the tumor cells infiltrates. The area (µm<sup>2</sup>) was calculated from the stained slides, selecting the follicles. Eight follicles were analyzed for each slide, and the experimental group and the results were expressed as average and SDs of infiltrated tumor cells area (µm<sup>2</sup>). Analyses were done by a pathologist and a hematopathologist and then averaged.

**Immunohistochemistry.** Deparaffinized 4-µm spleen sections were incubated sequentially in accordance with the instructions of the LSAB kit from DAKO Corporation. Antigen retrieval was done by immersing the slides in 0.01% sodium citrate (pH 6.0) incubated for 5 min in boiling water. The endogenous peroxidase activity was inhibited by immersing the slides in 3% H<sub>2</sub>O<sub>2</sub>-methanol for 25 min, and the background nonspecific binding was reduced by incubating with 1% bovine serum albumin in PBS for 60 min. The slides were incubated overnight at room temperature with the human-specific antibody against CD20 (1:100; Santa Cruz). Finally, the slides were washed five times in 0.1 mol/L PBS (pH 7.4) for 8 min. To reduce the variability, all samples from each group were processed at the same time in a single experiment using a single batch of antibody diluted in PBS-bovine serum albumin. After washing, the slides were incubated with a biotinylated secondary antibody container in the LSAB kit from DAKO corporation for 30 min at room temperature followed by an incubation with a streptavidin-horseradish peroxidase conjugate container in the LSAB kit for 30 min at room temperature, and then with 3,3'-diaminobenzidine tetra-hydrochloride (liquid 3,3'-diaminobenzidine, DAKO Corporation) for 1 to 6 min in the dark. The reaction was arrested with distilled water and the slides were counterstained with hematoxylin. Thereafter, the tissues were washed in tap water for 5 min., dehydrated through ethanol baths (70%, 90%, and 100%) in xylene, and mounted with E-2 Mount medium (Shandon Lab). Finally, the slides were analyzed under light microscopy (Olympus BX-40).

**In situ detection of DNA fragmentation (terminal deoxynucleotidyl transferase-mediated dUTP nick end labeling).** Tissue tumor samples were embedded in paraffin, and 3- to 5-µm slices were cut with a microtome and placed on coated slides, paraffin was removed from the tissue sections with xylene, and the sections were rehydrated in graded ethanol solutions. DNA fragmentation was detected by the terminal deoxynucleotidyl transferase-mediated dUTP nick end labeling (TUNEL) method. After the tissue sections were deparaffinized, the slides were immersed in 0.01% sodium citrate (pH 6.0) incubating for 20 min in boiling water. The endogenous peroxidase activity was inhibited by immersing the slides in 3% H<sub>2</sub>O<sub>2</sub>-methanol for 25 min. The slides were incubated for 1 h in 37°C with the TdT enzyme of the TUNEL kit (Roche). After three washes in PBS 0.1 mol/L (pH 7.4) for 5 min, the slides were incubated with POD solution for 30 min in 37°C after washing, and the color was developed with 3,3'-diaminobenzidine tetra-hydrochloride (liquid DAB, DAKO Corporation) for 1 to 5 min in the dark. The reaction was arrested with distilled water and the slides were counterstained with hematoxylin. Thereafter, the tissues were washed in tap water for 5 min, dehydrated through ethanol baths (70%, 90%, and 100%) in xylene and mounted with E-2 Mount medium (Shandon Lab). Finally, the slides were analyzed under light microscopy (Olympus BX-40).

#### **Statistical analysis**

All results were expressed as the mean ± SD of data obtained from three to four separate experiments. The statistical significance of the differences between group means was determined using one-way ANOVA to compare variance. Significant differences were considered for probabilities of <5% ( $P < 0.05$ ).

## **Results**

**Rituximab-mediated biological activities (except CDC and ADCC) are Fc independent.** We have reported that rituximab triggers CD20<sup>+</sup> B-NHL cells and results in the inhibition of several intracellular survival pathways leading to chemo/immunosensitization (11–13). Cell signaling by rituximab might have resulted from both the direct triggering of the CD20 receptor on tumor cells and by coengagement of the Fc receptor on tumor cells through the Fc-binding region of rituximab. The impact of Fc binding on rituximab-mediated cell signaling was examined using CH2<sup>-</sup> (the Fc-binding domain) deleted rituximab and by rituximab (Fab')<sub>2</sub> fragments. To investigate these possibilities, the role of Fc was examined by abolishing the properties of both genetically engineered (CH2<sup>-</sup>) rituximab and rituximab (Fab')<sub>2</sub> fragments.

Cell surface binding of the various antibodies to B-NHL cell lines was examined by flow cytometry. Treatment of the four B-NHL cell lines (2F7, Raji, Ramos, and Daudi) with rituximab showed significant binding to all cell lines and the mean fluorescence intensity was significantly augmented compared with the control IgG used. By comparison, using the same molar concentrations, rituximab (CH2<sup>-</sup>), rituximab (CH2<sup>-</sup>) Dimer, and rituximab (Fab')<sub>2</sub> stained all four cell lines and the mean fluorescence intensity was in the same range as those observed with the native rituximab molecule (Supplementary Table S1).

The activities of rituximab (Fab')<sub>2</sub> and genetically engineered CH2<sup>-</sup> deleted rituximab molecules [monomeric rituximab (CH2<sup>-</sup>) and rituximab (CH2<sup>-</sup>) Dimer] were compared with those of unmodified native rituximab. The CH2 domain has been shown to exert several of the effector functions of the Fc fragment of antibody molecules such as its involvement in mediating both

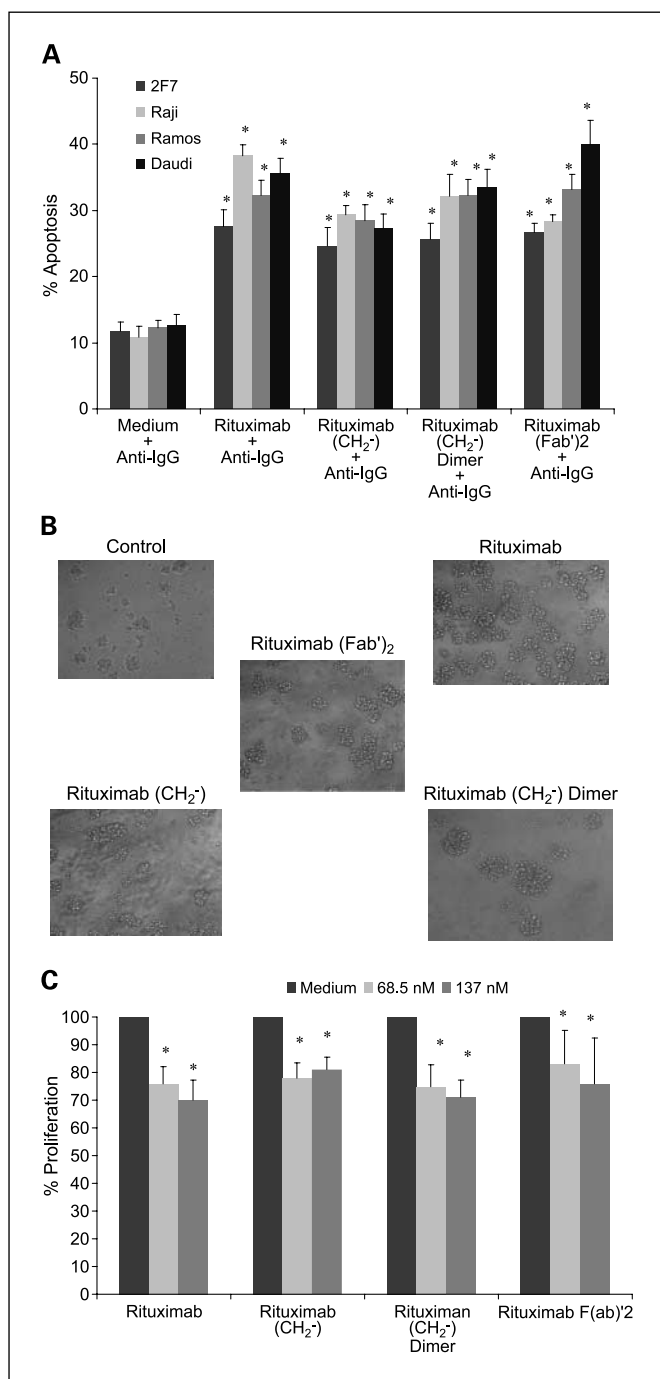


**Fig. 1.** Induction of apoptosis, cell aggregation, and inhibition of proliferation by rituximab (CH<sub>2</sub>), rituximab (CH<sub>2</sub>) Dimer, and rituximab (Fab')<sub>2</sub>. **A**, apoptosis. Tumor cells ( $2 \times 10^6$ /mL; 2F7, Raji, Ramos, and Daudi) were incubated overnight at 37°C with rituximab, rituximab (CH<sub>2</sub>), rituximab (CH<sub>2</sub>) Dimer, and rituximab (Fab')<sub>2</sub> at the concentration of 137 nmol/L alone or cross-linked with goat anti-human IgG (342.5 nmol/L), and the cells were then evaluated for apoptosis for the presence of active caspase-3 (\*,  $P < 0.001$ ). **B**, cell aggregation. The 2F7 tumor cells ( $1 \times 10^6$ ) were treated with 137 nmol/L of the different rituximab molecules. The cells were then visualized on an inverted microscope and the images were captured and analyzed using Adobe Photoshop 3.0.5 and a Sony DKC-5000 digital camera. **C**, proliferation. The 2F7 cells ( $1 \times 10^6$ /mL) were cultured in the absence or the presence of rituximab molecules at concentrations of 68.5 and 137 nmol/L for 24 h at 37°C. The cells were recovered and viability was determined microscopically by trypan blue dye exclusion. The number of viable cells was recorded and the data were analyzed by determining percent of control of cells cultured in medium alone (\*,  $P < 0.001$ ).

CDC and ADCC (14). Rituximab mediated a very significant CDC activity, which was dependent on the antibody concentration used and reached a maximum cytotoxicity of ~80% (Supplementary Fig. S3A). As expected, both rituximab (CH<sub>2</sub>) and rituximab (CH<sub>2</sub>) Dimer showed no CDC activity at any of the antibody concentrations used, which was similar to the baseline observed with the IgG isotype control (Supplementary Fig. S3A). In addition, lack of CDC activity by rituximab (Fab')<sub>2</sub> was also confirmed in an independent experiment (Supplementary Fig. S3B). Further, ADCC activity was examined by using human peripheral blood as effector cells and radiolabeled target cells as described in Materials and Methods. Rituximab exerted significant ADCC activity, and the percent-specific lysis was a function of the antibody concentration used. In contrast, both rituximab (CH<sub>2</sub>) and rituximab (CH<sub>2</sub>) Dimer did not show any ADCC activity above the control IgG levels (Supplementary Fig. S3C). These findings corroborate the CDC and ADCC functional properties of the CH<sub>2</sub> domain and show that the Fc effector functions are lost by the rituximab-modified molecules.

We next examined the ability of the various rituximab molecules to induce apoptosis when used alone or following cross-linking with secondary anti-human IgG. Treatment with various rituximab antibodies alone did not induce any significant apoptosis in all of the four cell lines (2F7, Raji, Ramos, and Daudi) tested. Previous studies have shown that cross-linking of monomeric rituximab results in induction of apoptosis in several cell lines (22). Thus, we examined the ability of the rituximab molecules to induce apoptosis following cross-linking with anti-human IgG antibody as described in methods. The modified rituximab exerted significant apoptosis in all of the four cell lines tested compared with cells treated with anti-IgG alone. The extent of apoptosis of both modified and unmodified rituximab molecules was comparable for all four lines tested (Fig. 1A). We selected to use 2F7 B-cell line as a representative for subsequent experiments. Treatment of B-NHL cell lines with rituximab results in significant homotypic aggregation of the tumor target cells (23). Like rituximab, the modified rituximab antibodies induced significant aggregation of 2F7 cells (Fig. 1B) and other B-NHL cell lines tested (data not shown). Further, treatment of the 2F7 B-NHL cell line with rituximab or with modified rituximab antibodies resulted in significant inhibition of cell growth and the extent of inhibition was approximately equal for all four antibody molecules (Fig. 1C).

Altogether, the above findings show that although, as expected, the modified rituximab molecules have lost their Fc-mediated ADCC and CDC effector functions, they retained other antibody-mediated effects such as binding to CD20, induction of apoptosis following cross-linking, cell aggregation, and inhibition of cell growth.

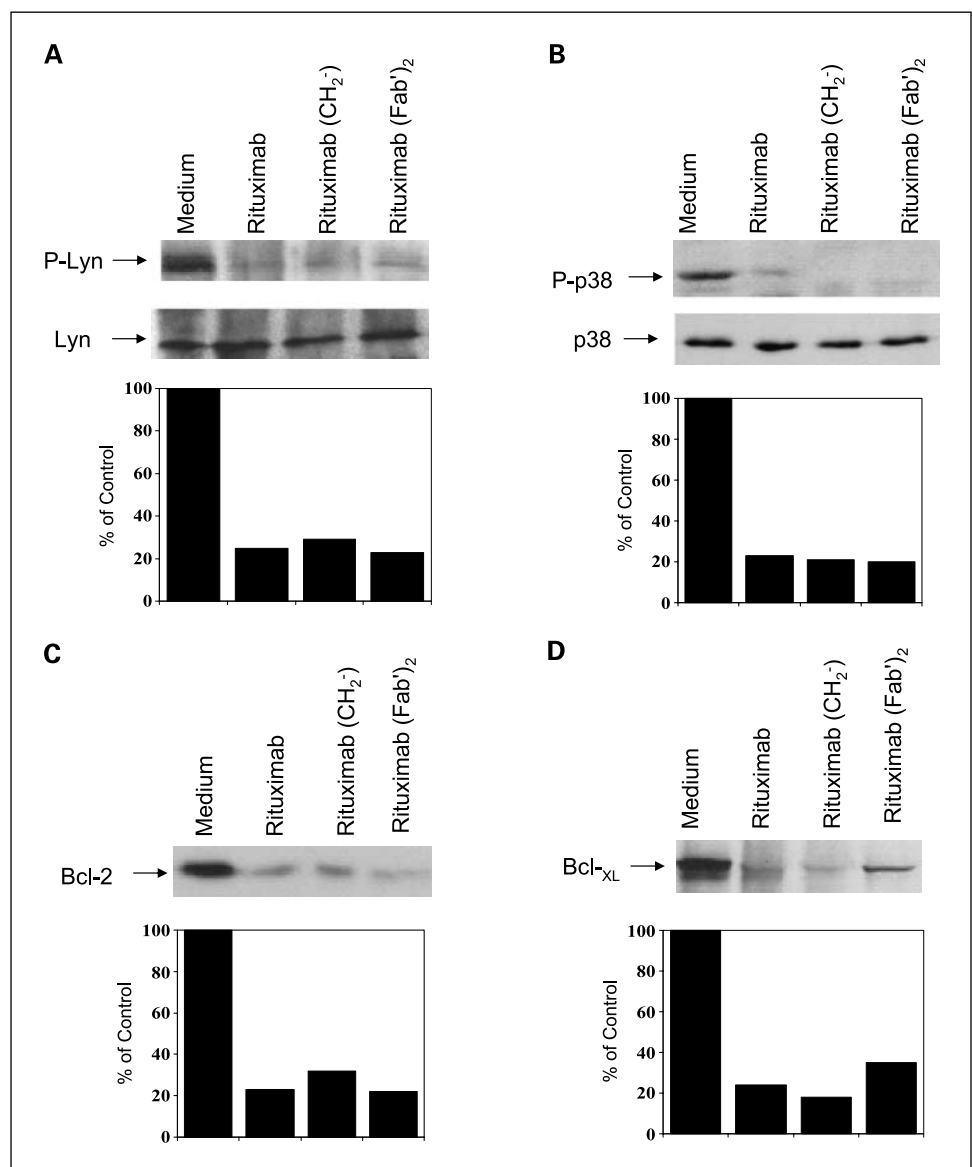
**Independence of Fc for rituximab-mediated inhibition of cell survival signaling pathways.** We have reported that rituximab triggers B-NHL cell lines and modifies several intracellular signaling pathways such as the p38 MAPK and the NF- $\kappa$ B pathways in both AIDS NHL (10, 24) and non-AIDS NHL (24). These molecular signaling pathways were inhibited by rituximab and resulted in the selective downregulation of anti-apoptotic resistant factors such as Bcl-2 and Bcl-x<sub>L</sub> and consequently led to sensitization of the resistant tumor cells to drug-mediated apoptosis. Because the B-NHL cell lines express Fc receptors and *in vivo* rituximab-treated cells interact

with host FcR-bearing cells, it was plausible that rituximab-mediated signaling in B-NHL cells lines may have resulted not only from direct triggering of CD20 but by the cooperation of the Fc fragments of rituximab interacting with tumor surface Fc receptors. These possibilities were addressed by comparing rituximab with (Fab')<sub>2</sub> antibodies in the inhibition of cell signaling pathways. We examined representative gene products in the survival signaling pathways that are modified by rituximab as well as several transcription factors that are regulated by such survival pathways. Rituximab inhibited the Src-kinase p-Lyn, but not Lyn, and a similar inhibition was also observed by the modified antibodies (Fig. 2A). Likewise, the p-p38 MAPK activity, but not p38 MAPK, was also significantly inhibited by the modified rituximab antibodies (Fig. 2B). Inhibition of the p38 MAPK activity by the modified antibodies, such as rituximab, resulted in the inhibition of Bcl-2 in the 2F7 cell line (10) and Bcl-xL expression in Ramos (Bcl-2 deficient; refs. 13, 22), and the extent of the inhibition was the same for ritux-

imab and the modified antibodies (Fig. 2C and D). Inhibition by rituximab of the p38 MAPK pathway also results in the inhibition of the NF-κB pathway as well as STAT-3-mediated activity (10). Thus, we examined the transcription factors regulated by the activation of p38 MAPK pathway and found that both native and modified antibodies significantly inhibited the activities of the transcription factors NF-κB (Fig. 3A), YY1 (the transcription factor Yin Yang 1; Fig. 3B), SP-1 (Fig. 3C), and STAT-3 (Fig. 3D) as assessed by electrophoretic mobility shift assay. The extent of inhibition was the same for all of the antibody molecules used at equivalent concentrations. The specificity of rituximab-mediated inhibition of the transcription factors was shown by failure of rituximab to inhibit the transcription factor AP-2 (Supplementary Fig. S3D).

Altogether, the above findings show that rituximab signals the cells directly via its interaction with the CD20 receptor and there was no detectable contribution from the Fc fragment of rituximab.

**Fig. 2.** Inhibition of the p38 MAPK pathway and downregulation of Bcl-2 or Bcl-xL expression by rituximab, rituximab (CH<sub>2</sub>), and rituximab (Fab')<sub>2</sub>. The 2F7 and Ramos tumor cells were cultured with 137 nmol/L of the different rituximab molecules for 24 h at 37°C and lysates were prepared as described in Materials and Methods. The lysates from 2F7-treated cells were then analyzed for the presence of Lyn and p-Lyn (A), p38 MAPK, p-p38 MAPK (B), and for Bcl-2 (C). Lysates from Bcl-2-deficient Ramos were analyzed for Bcl-xL (D). The Western blots were analyzed by densitometry to show the relative levels of the proteins compared with levels in untreated cells. The data are representative of two similar experiments.



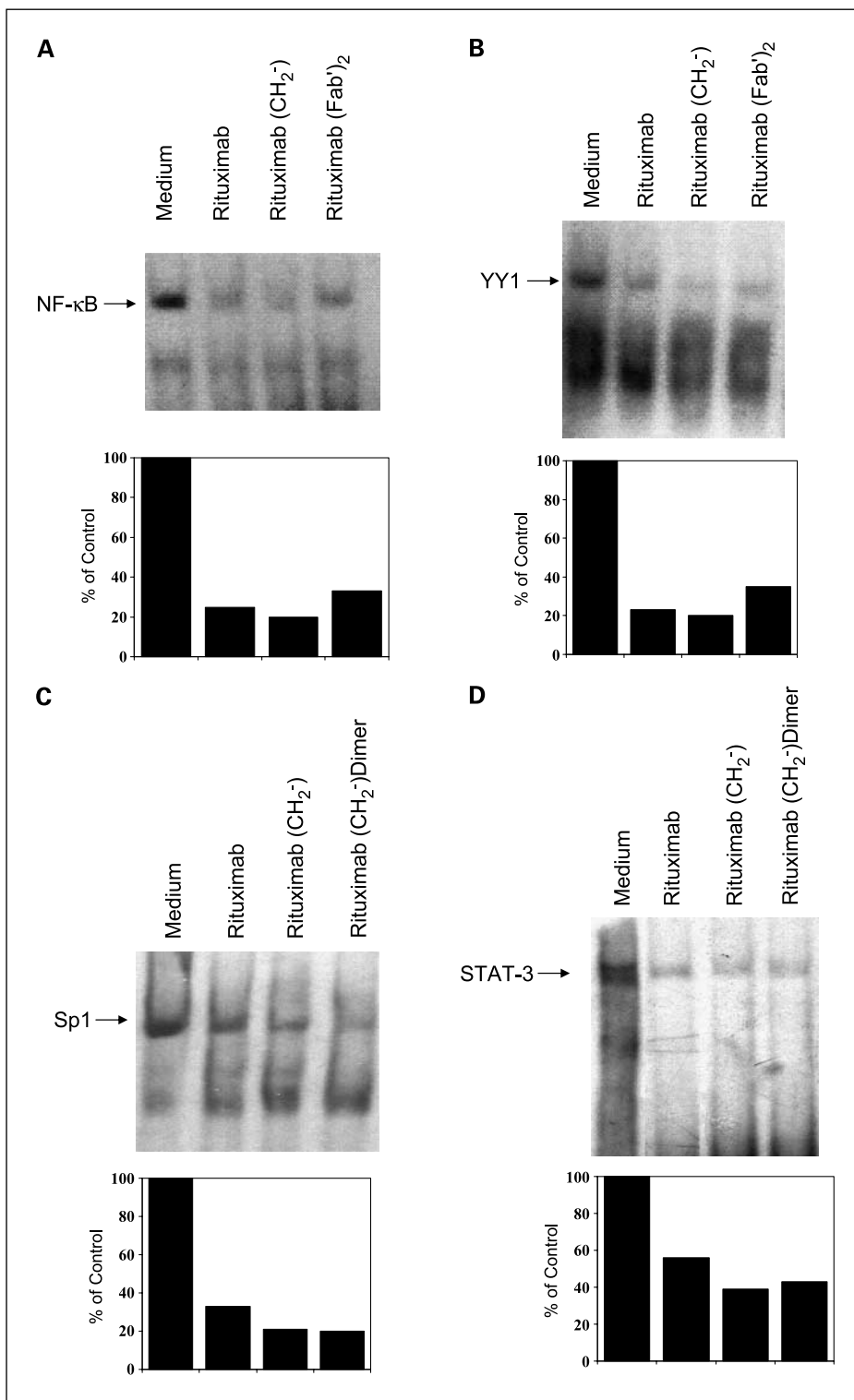


**Fig. 3.** Inhibition of NF- $\kappa$ B, Sp1, YY1, and STAT-3 DNA-binding activities by rituximab, rituximab (CH<sub>2</sub>'), and rituximab (Fab')<sub>2</sub>. 2F7 cells were treated with 137 nmol/L of the rituximab molecules for 24 h at 37°C. Nuclear lysates were prepared and were tested by electrophoretic mobility shift assay for NF- $\kappa$ B (A), YY1 (B), Sp1 (C), and STAT 3 (D). The data were analyzed by densitometry and plotted for percent relative expression compared with control cells (100%). The specificity of the electrophoretic mobility shift assay analysis was shown by using AP-2 (S3D) (E) DNA-binding activity that is not affected by rituximab.

**Chemosensitization and immunosensitization of B-NHL cell lines by rituximab are Fc independent.** We have previously reported that rituximab sensitizes resistant B-NHL cell lines to apoptosis by both chemotherapeutics and immunotherapeutics. Hence, because we have shown above that the Fc-deficient antibody inhibited Bcl-2/Bcl-x<sub>L</sub> expression and these were shown to be responsible for resistance, we examined the abil-

ity of modified antibodies to sensitize B-NHL cell lines to apoptosis (10–12, 25). Treatment of 2F7 cells with rituximab, rituximab (CH<sub>2</sub>'), rituximab (CH<sub>2</sub>') Dimer, and rituximab (Fab')<sub>2</sub> significantly sensitized the 2F7 cells to CDDP-induced apoptosis. There was modest apoptosis by treatment with single agents. The extent of sensitization was the same by all 4 rituximab antibody molecules used at equivalent molar

concentrations (Fig. 4A). Similar findings were also observed with the other cell lines (Raji, Ramos, and Daudi) where significant sensitization to CDDP-induced apoptosis was also observed by all four antibodies (Supplementary Table S2).

In addition to chemosensitization, we have also reported that rituximab treatment of B-NHL cell lines induces upregulation of Fas expression and sensitizes the tumor cells to Fas ligand-induced apoptosis (11, 12). Immunosenitization was dependent on rituximab-induced inhibition of NF- $\kappa$ B and YY1 and we have shown here that the modified rituximab antibodies

also inhibited these transcription factors (Fig. 3). Hence, immunosenitization to FasL was examined with the modified antibodies. The findings show that all of the modified antibodies induced significant upregulation of cell surface Fas expression in all four B-NHL cell lines tested (2F7, Raji, Ramos, Daudi) as assessed by flow cytometry. There was significant enhancement of the mean fluorescence intensity in the antibody treated cells compared with treatment with control IgG (Supplementary Table S3). In addition, the Fas ligand agonist antibody, CH-11, was found to be cytotoxic following treatment of the

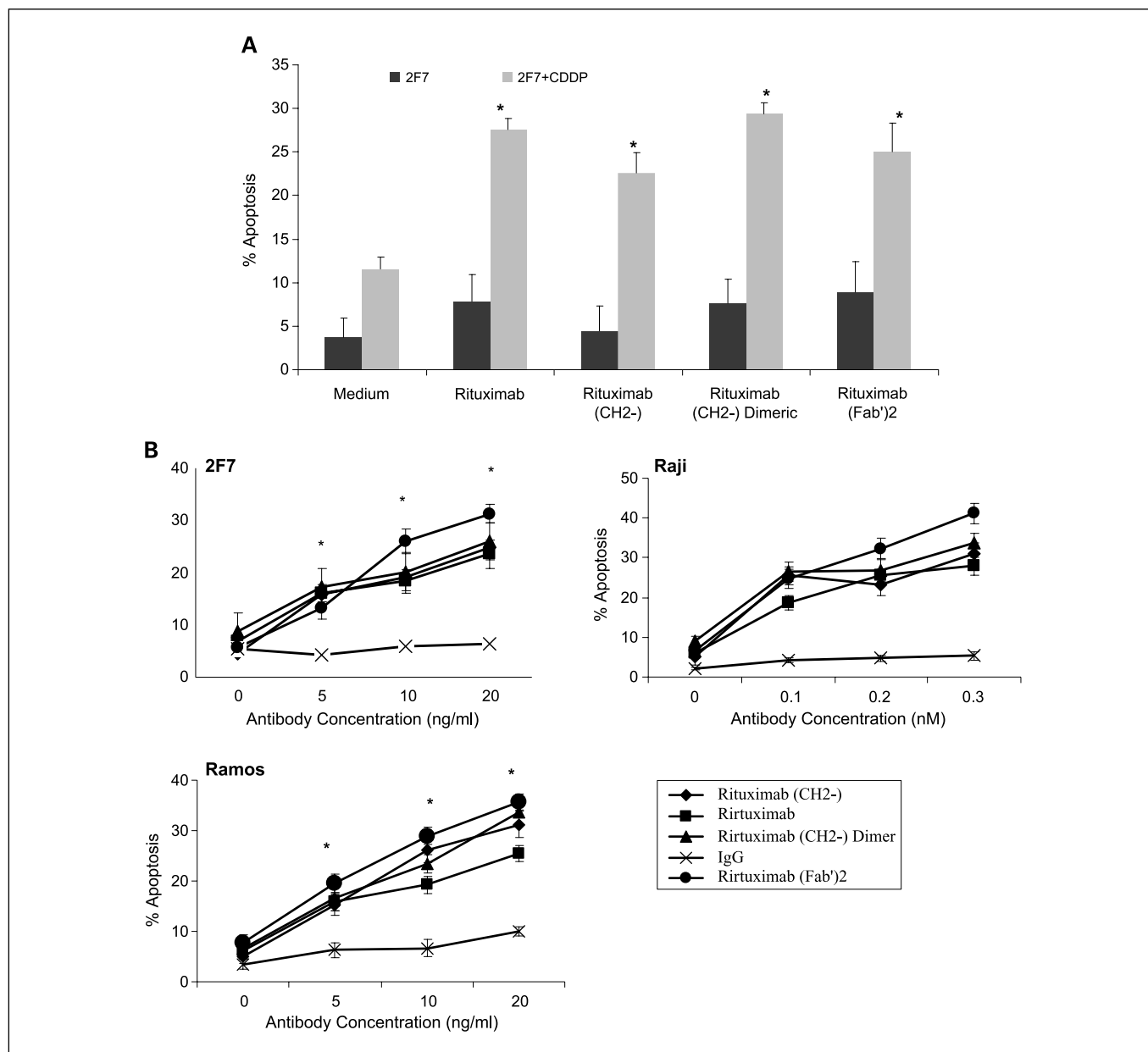


**Fig. 4.** Chemosensitization and immunosenitization of 2F7 cells by rituximab, rituximab CH<sub>2</sub><sup>-</sup>, rituximab CH<sub>2</sub><sup>-</sup> Dimer, and rituximab (Fab')<sub>2</sub>. **A**, rituximab-induced chemosensitization to CDDP. 2F7 cells ( $1 \times 10^6$ /mL) were incubated with CDDP (5  $\mu$ g/mL) alone or in combination with 137 nmol/L of rituximab molecules. The cells were incubated for 24 h at 37°C and analyzed for active caspase-3 for apoptosis by flow as described in Materials and Methods (\*,  $P < 0.01$ ). **B**, rituximab-induced sensitization to CH-11 apoptosis. The tumor cells ( $1 \times 10^6$ /mL; 2F7, Raji, and Ramos) were treated with 137 nmol/L rituximab CH<sub>2</sub><sup>-</sup>, rituximab CH<sub>2</sub><sup>-</sup> Dimer, and rituximab (Fab')<sub>2</sub> or control IgG1 for 18 h, alone or in combination with different concentrations of the Fas ligand agonist antibody CH-11. The cells were then analyzed for active caspase-3 for apoptosis as described in Materials and Methods and the percentage of apoptotic cells was determined (\*,  $P < 0.05$ ).



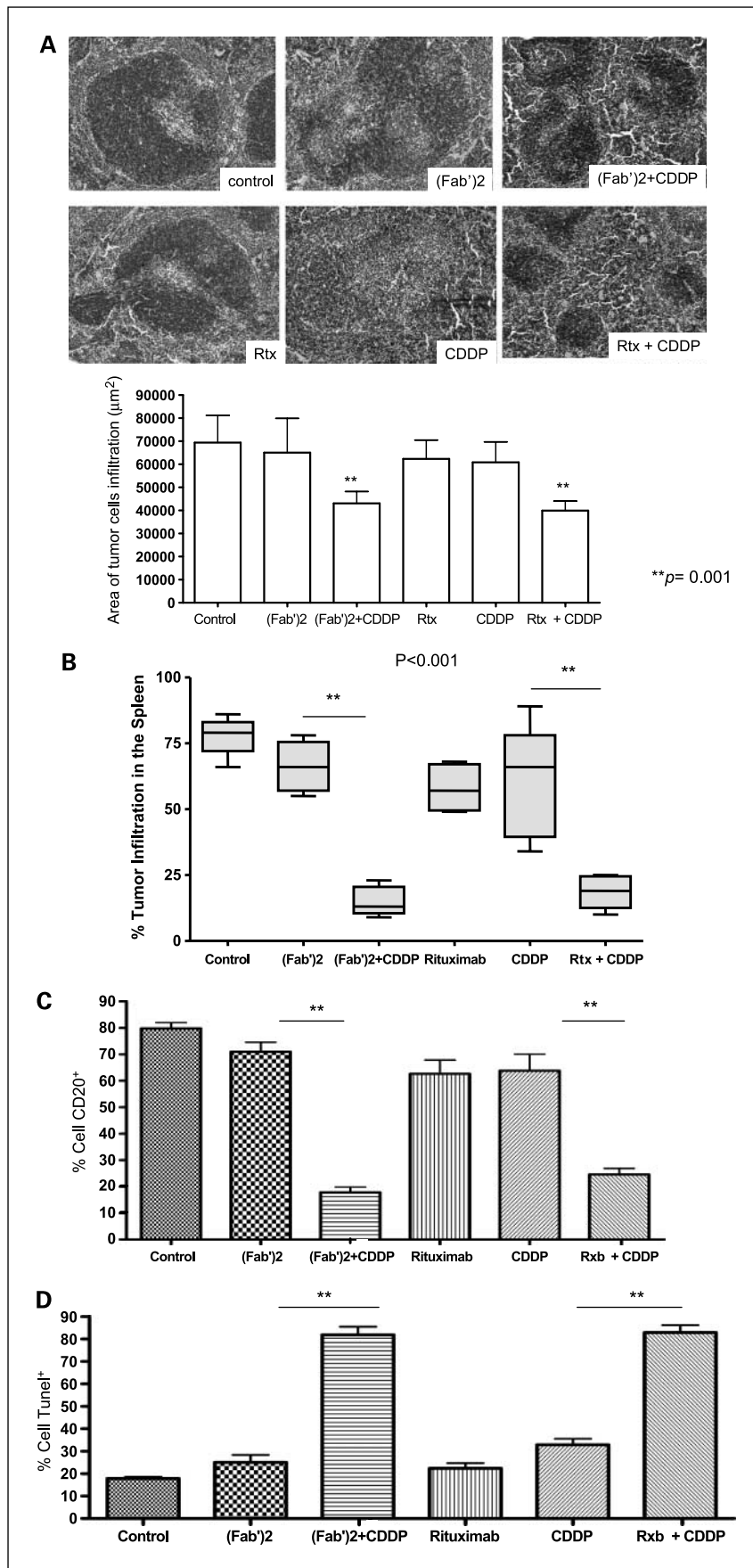


**Fig. 5.** *In vivo* inhibition of Raji tumor cell growth by rituximab (Fab')<sub>2</sub> in combination with CDDP. The ability of rituximab (Fab')<sub>2</sub> antibody to suppress tumor infiltration was examined in an established lymphoma xenograft mouse model as described in Materials and Methods. Raji cells were inoculated i.p. into the mice. Treatment started 8 d after tumor cell inoculation by i.p. injection of 100  $\mu\text{g}$  rituximab or rituximab (Fab')<sub>2</sub>, and 1 and 2 d later, the mice were inoculated with CDDP (4 mg/Kg) for two cycles at 10-d intervals. Five mice were used for each treatment group. The mice were sacrificed on day 60. **A**, immunohistochemical analysis of H&E staining of spleen cells from each representative group. Representative images for each group are shown. The area of tumor cells infiltration is plotted. \*\*,  $P < 0.001$  significant differences between the group treated with antibodies and CDDP compared with group treated with antibodies alone. **B**, the percent tumor infiltration in spleens is depicted by box plots. The line inside each box denotes median. \*\*,  $P < 0.001$ , comparing tumors treated with antibodies and CDDP to tumors treated with antibodies alone. **C**, the percent of CD20-positive apoptotic cells was detected by TUNEL. **D**, representative tumor cell infiltration in the spleens of treated mice. Tumor areas (follicles) were randomly selected for analysis and were plotted. Columns, mean; bars, SEM. \*\*,  $P < 0.001$ , comparing the group treated with antibodies and CDDP with the group treated with antibodies alone.

tumor cells (2F7, Raji, and Ramos) with the modified antibodies, and the level of sensitization was a function of the CH-11 antibody concentration used (Fig. 4B).

Altogether, the above findings show that, such as rituximab, rituximab CH<sub>2</sub> or rituximab (Fab')<sub>2</sub> sensitize B-NHL cell lines to both the CDDP chemotherapeutic drug and to the Fas ligand-induced apoptosis. These results also suggest that chemosensitization and immunosensitization by rituximab *in vivo* can be Fc-independent.

**In vivo therapeutic effect of rituximab (Fab')<sub>2</sub> in combination with CDDP on Raji tumor xenografts.** Nude mice were inoculated i.p. with Raji cells and treated with rituximab, rituximab (Fab')<sub>2</sub>, CDDP, and combinations as described in Materials and Methods. The mice were sacrificed at day 60 and their spleens were removed and analyzed. A representative immunohistochemical analysis of tumor cell infiltrates in the spleen of mice following various treatments is shown in Fig. 5A. Clearly, in contrast to single agent treatment, the combination treatment of rituximab plus CDDP or rituximab (Fab')<sub>2</sub> plus CDDP reduced significantly the area of tumor cell infiltrates. The data in Fig. 5B show that untreated mice had 75 ± 8.6% tumor infiltrates. Treatment with single-agent rituximab, rituximab (Fab')<sub>2</sub>, or CDDP did not have any significant effect on the percent of tumor infiltrate compared with untreated mice. In contrast, treatment with the combination of rituximab plus CDDP or rituximab (Fab')<sub>2</sub> plus CDDP resulted in significant inhibition of tumor cell infiltrates ( $P < 0.001$ ). The combination treatment reduced tumor infiltrates from a mean of 75% to a mean of 18% (four fold reduction). These findings show the therapeutic effect of the combined treatment on tumor growth.

The tumor infiltrates were further examined by staining with a specific human anti-CD20 antibody to directly examine Raji tumor cell infiltrates. The findings corroborated those obtained above using the immunohistochemical staining. Control, untreated mice had a mean of 80% CD20-positive cells,

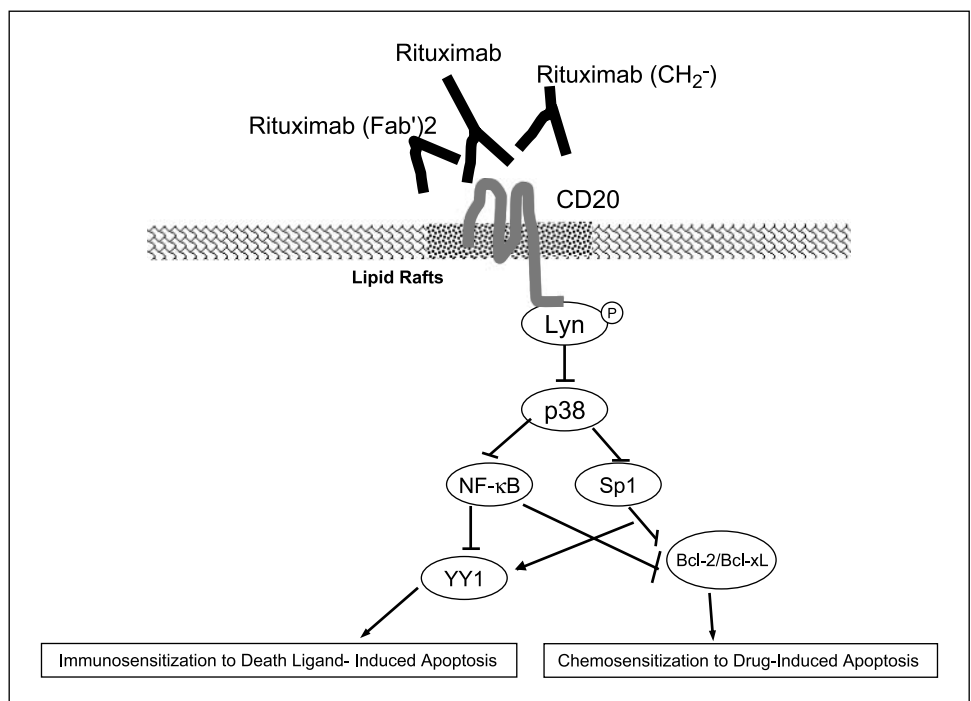
and treatment with single agents rituximab, rituximab (Fab')<sub>2</sub>, or CDDP did not have any significant inhibition on tumor infiltrates. However, the combination treatment of both rituximab (Fab')<sub>2</sub> plus CDDP or rituximab plus CDDP reduced the frequency of CD20-positive cells to a mean of 20%, a 4-fold reduction (Fig. 5C).

The *in vitro* analysis shown in Fig. 4A showed that the combination treatment of rituximab or rituximab (Fab')<sub>2</sub> plus CDDP resulted in significant induction of apoptosis. Thus, we examined if the combination treatments *in vivo* in mice also resulted in the induction of apoptosis in the tumor cells. The spleen cells derived from the mice were examined for apoptosis by the TUNEL assay as described in Materials and Methods. The findings in Fig. 5D show clearly that antibody treatment did not show any apoptosis compared with control. Treatment with CDDP induced a slight increase (~15%) of apoptotic cells above control and antibody treatment. However, the combination treatment of rituximab plus CDDP or rituximab (Fab')<sub>2</sub> plus CDDP resulted in significant potentiation in the frequency of apoptotic cells (80%). Here again, there was 4-fold increase above controls following the combination treatment. Altogether, these findings show that the combination treatment results in significant inhibition of tumor cell infiltrates in the spleen as well as the induction of apoptosis. Further, there were no differences between treatments with rituximab or rituximab (Fab')<sub>2</sub>.

## Discussion

We have reported that rituximab can trigger B-NHL cell lines *in vitro* and modify several intracellular signaling pathways that result in reversing the chemoresistant and immunoresistant phenotypes to sensitive phenotypes. These studies did not address whether rituximab directly triggers the cells via the CD20 receptor in the absence of any additional costimulation via the

**Fig. 6.** Schematic diagram illustrating the cell signaling and chemo/ immunosensitizing effects of rituximab, rituximab CH<sub>2</sub>, and rituximab (Fab')<sub>2</sub> following treatment of B-NHL cell lines. The diagram shows that the various rituximab antibody molecules [rituximab, rituximab CH<sub>2</sub>, rituximab CH<sub>2</sub> Dimer and rituximab (Fab')<sub>2</sub>] can directly trigger the cells via CD20 and inhibit the p38 MAPK and NF- $\kappa$ B signaling pathways, leading to inhibition of YY1 (shown to regulate the resistance to Fas L) and the antiapoptotic gene products Bcl-2/Bcl-x<sub>L</sub> (shown to regulate resistance to chemotherapeutic drugs) and resulting in both chemo and immunosensitization, respectively.



Fc fragment of rituximab and Fc receptors expressed on the tumor cells. The present findings provide evidence that rituximab-mediated biological activities (except ADCC and CDC) and cell signaling are Fc independent as corroborated by the use of rituximab (Fab')<sub>2</sub> and genetically engineered CH2-depleted rituximab. The various functions examined with the modified antibodies were conserved and were comparable with unmodified rituximab such as the ability to inhibit cell proliferation, induce cell aggregation, induce apoptosis following cross-linking with a secondary anti-IgG antibody, and to inhibit the constitutively activated p38 MAPK and NF-κB signaling pathways. In addition, the various antibodies were comparable in their ability to sensitize resistant tumor cells to both chemotherapeutic drugs and Fas ligand-induced apoptosis. *In vivo* studies in mice showed the therapeutic efficacy of rituximab (Fab')<sub>2</sub> in combination with CDDP, and was similar to rituximab plus CDDP, as determined by inhibition of tumor growth. These findings show that cell signaling observed *in vitro* by rituximab results primarily from the direct trigger of the CD20 receptor in the absence of any contribution from the Fc region of anti-CD20 antibody and can also take place *in vivo* in an Fc-independent manner. The findings suggest that the *in vivo* observed chemosensitization and immunosensitization following rituximab treatment may still take place in individuals who have reduced Fc-dependent effector functions such as ADCC and CDC activities (26) and in patients expressing low affinity variant of Fc-receptors due to polymorphism (6, 27).

Several studies have identified the CH2 domain of the IgG antibody molecule to mediate effectors functions such as its role in ADCC and CDC (28, 29). This was corroborated with the genetically engineered monomeric rituximab (CH2<sup>-</sup>) and rituximab (CH2<sup>-</sup>) Dimer that were found to be devoid of any ADCC and CDC activities. These modified antibodies bind the corresponding CD20 receptor on the surface of B-NHL cell lines similar to rituximab. In contrast to their deficiencies in CDC and ADCC, the CH2-deleted and (Fab')<sub>2</sub> antibodies significantly inhibited cell growth and induced apoptosis following cross-linking with anti-IgG antibodies. These various effects, therefore, are independent of the Fc fragment and do not require cross-linking of the Fc fragment of rituximab with Fc receptor-bearing B-NHL cells. The present findings are in agreement with those of Carderelli et al. (30) who have reported that an (Fab')<sub>2</sub> fragment of anti-CD20 B1 antibody can induce apoptosis.

We have reported previously that rituximab can trigger B-NHL cell lines and modify several intracellular signaling pathways that result in sensitization of the drug-resistant tumor cells to drug-induced apoptosis (10, 24, 27). It was possible that the molecular signaling triggered by rituximab might have been the result of cooperation between the rituximab-CD20 receptor interaction and the interaction between the Fc fragment of rituximab and Fc receptors on the target cells. Clearly, Fc receptors can be triggered for signaling depending on the type of the Fc receptor expressed on the cells. Fc-γ receptor stimulation may lead to either activation or inhibition of cell signaling (31, 32). For example, the Fc-receptors Fc-γRIII/CD16A are expressed on NK cells, macrophages, and a subset of T-cells, and trigger ADCC. Cross-linking of CD16A on NK cells, by immune complexes or by an anti-CD16 antibody, for example, initiates a cascade of signaling events including the tyrosine phosphorylation of the γ chain (33) and other proteins, intracellular calcium mobilization, and activation of

phospho-lipases A2, C, and D. Activation of CD16A is coupled directly or indirectly by a nonreceptor tyrosine kinase. This inference is confirmed in studies in which the tyrosine phosphorylation of kinases including p72Syc p56lck, Shc, and p36 and activation of phosphatidylinositol 3-kinase have been observed (34). Also, cross-linking of FcγRIII resulted in significant levels of p38MAPK phosphorylation (35). The inhibitory Fc-γRIIB receptor is a single-chain molecule that carries an ITIM motif in its cytoplasmic domain and functions through recruitment of the inositol phosphatase SHIP through binding to an SH2 site generated on the Fc-γRIIB ITIM. With the exception of T cells and NK cells, Fc-γRIIB is expressed in all cells of the immune system and it is the only receptor on B cells where it regulates activity by signals delivered by immune complexes of the B-cell receptor. When coligated with BCR, it triggers two ITIM-dependent signaling pathways that inhibit cell proliferation and cell activation (16). Thus, these various Fc-receptor-mediated signaling pathways might have contributed to our observed findings of rituximab-mediated inhibition of cell signaling. Our approach to rule out the role of FcR cross-linking in rituximab-mediated inhibition of cell signaling, we investigated tumor cell triggering by functionally defective Fc (CH2<sup>-</sup>) and (Fab')<sub>2</sub> rituximab antibodies and compared the findings with the native rituximab. Rituximab triggers the 2F7 B-NHL line and dephosphorylates p38 MAPK and STAT-3 and also inhibits Bcl-2/Bcl-x<sub>L</sub> expression (10, 24, 36). In this study, we show that the CH2<sup>-</sup> and the (Fab')<sub>2</sub> antibodies were able to trigger the cells and modify the above pathways such as rituximab. These findings exclude the role of Fc in rituximab-induced cell triggering and inhibition of survival pathways.

We have found that the CH2-deleted and (Fab')<sub>2</sub> antibodies behave such as rituximab in their ability to sensitize resistant tumor cells to chemotherapy and Fas ligand-induced apoptosis. Inhibition of Bcl-2 expression in 2F7 cells was responsible, in large part, for chemosensitization (23). Our findings with the modified rituximab showed that inhibition of Bcl-2/Bcl-x<sub>L</sub> expression was similar to that obtained by rituximab; thus, the modified antibodies can sensitize the tumor cells to CDDP-induced apoptosis. In addition to chemosensitization, rituximab can also sensitize B-NHL cell lines to Fas ligand-induced apoptosis. This was the result of rituximab-mediated upregulation of Fas expression via inhibition of NF-κB and the transcription repressor YY1 (11, 12). We have previously reported that YY1 regulates the expression of Fas via DNA binding to the silencer region of the Fas promoter (37). Inhibition of YY1 relieves the repression and Fas transcription is upregulated. In the present study, we also show that the modified antibodies, such as rituximab, inhibited YY1 DNA-binding activity and resulted in the upregulation of Fas expression and sensitization to CH-11-induced apoptosis.

The *in vitro* findings discussed above showed clearly that chemosensitization can take place by (Fab')<sub>2</sub>-treated Raji cells. *In vivo*, the role of effector cells bearing FcRs such as purified NK cells in the sensitization of tumor cells by rituximab (Fab')<sub>2</sub>-treated cells was not clear. Thus, we examined the role of purified NK cells derived from normal PBMCs on the chemosensitization effect of rituximab (Fab')<sub>2</sub> to CDDP. The data showed clearly that NK cells had no effect on rituximab (Fab')<sub>2</sub>-treated cells in the presence of CDDP and the cytotoxicity obtained resulted primarily from the sensitizing

effect mediated by rituximab (Fab')<sub>2</sub>, and there was no additional effect by the NK cells (Supplementary Fig. S6). These findings suggest that host FcR-bearing effector cells do not interfere with the sensitizing effect of rituximab (Fab')<sub>2</sub>-treated cells. However, they can have additive effects when the target cells are treated with rituximab in the presence of CDDP, via the additional roles of ADCC and CDC.

The findings achieved *in vitro* showed the equivalent sensitization of Raji cells by rituximab (Fab')<sub>2</sub> or rituximab for CDDP-induced apoptosis and were corroborated in an *in vivo* Raji tumor cell xenograft model. The *in vivo* data showed clearly the therapeutic efficacy of rituximab (Fab')<sub>2</sub> as a chemosensitizer and mimics rituximab with the same magnitude of tumor cell inhibition. These findings indicate the potential therapeutic efficacy of rituximab (Fab')<sub>2</sub> when combined with chemotherapy. It is not clear whether rituximab (Fab')<sub>2</sub> might result in a better therapeutic index in patients with B-NHL when combined with chemotherapy. It is possible that, *in vivo*, rituximab (Fab')<sub>2</sub> might have a faster clearance rate and reduce its therapeutic efficacy. Likewise, it is also possible that rituximab (Fab')<sub>2</sub> might reach tumor sites that are not reached by rituximab. Future studies will address these questions using different models of B-NHL xenografts.

The present findings clearly show that rituximab-mediated functions, cell signaling, and both chemosensitization and

immunosensitization are the result of the direct effect of the antibody binding to its cognate CD20 receptor, and these effects do not require the participation or cooperation of cross-linking rituximab Fc fragment with the Fc receptors on the tumor cells or on host cells *in vivo*. A schematic diagram representing the findings is shown in Fig. 6. In addition, the findings suggest that chemosensitization and immunosensitization by rituximab may be effective in poorly responding patients to rituximab treatment and who express low-affinity Fc  $\gamma$  receptors or those who may have defective ADCC or CDC activities. Such patients may benefit from the combination of rituximab and chemotherapeutic drugs or rituximab and TRAIL or anti-DR4/DR5 agonist antibodies.

### Disclosure of Potential Conflicts of Interest

The authors received a financial gift with no restrictions from Biogen/Dec Pharmaceuticals through the hospices of the Regents of the University of California.

### Acknowledgments

We thank Kate Dinh, Christine Yue, Tania Golkar, Maggie Yang, Erica Keng, and Tiffany Chin in the preparation of manuscript and Dr. Otoniel Martinez-Maza for valuable input and support.

### References

1. Reff ME, Carner K, Chambers S, et al. Depletion of B cells *in vivo* by a chimeric mouse human monoclonal antibody to CD20. *Blood* 1994;83:435-45.
2. Seymour JF. New treatment approaches to indolent non-Hodgkin's lymphoma. *Semin Oncol* 2004;31:27-32.
3. McLaughlin P, Grillo-Lopez AJ, Link BK, et al. Rituximab chimeric anti-CD20 monoclonal antibody therapy for relapsed indolent lymphoma: half of patients respond to a four-dose treatment program. *J Clin Oncol* 1998;16:2825-33.
4. Czuczman MS, Grillo-Lopez AJ, White CA, et al. Treatment of patients with low-grade B-cell lymphoma with the combination of chimeric anti-CD20 monoclonal antibody and CHOP chemotherapy. *J Clin Oncol* 1999;17:268-76.
5. Clynes RA, Towers TL, Presta LG, Ravetch JV. Inhibitory Fc receptors modulate *in vivo* cytotoxicity against tumor targets. *Nat Med* 2000;6:443-6.
6. Carton G, Dacheux L, Salles G, et al. Therapeutic activity of humanized anti-CD20 monoclonal antibody and polymorphism in IgG Fc receptor Fc $\gamma$ R1IIa gene. *Blood* 2002;99:754-8.
7. Weng WK, Levy R. Two immunoglobulin G fragment C receptor polymorphisms independently predict response to rituximab in patients with follicular lymphoma. *J Clin Oncol* 2003;21:3940-7.
8. Johnson P, Glennie M. The mechanisms of action of rituximab in the elimination of tumor cells. *Semin Oncol* 2003;30:3-8.
9. Pedersen IM, Buhl A, Klausen P, Geisler CH, Jurlander J. The chimeric anti-CD20 antibody rituximab induces apoptosis in B-cell chronic lymphocytic leukemia cells through a p38 mitogen activated protein-kinase-dependent mechanism. *Blood* 2002;99:1314-9.
10. Vega MI, Huerta-Yepez S, Garban H, Jazirehi A, Emmanouilides C, Bonavida B. Rituximab inhibits p38 MAPK activity in 2F7 B NHL and decreases IL-10 transcription: pivotal role of p38 MAPK in drug resistance. *Oncogene* 2004;23:3530-40.
11. Vega MI, Huerta-Yepez S, Bonavida B. Rituximab (anti-CD20) up-regulated Fas expression and sensitized B NHL to Fas mediated apoptosis. *Oncogene* 2005;24:8114-27.
12. Vega MI, Jazirehi AR, Huerta-Yepez S, Bonavida B. Rituximab-induced inhibition of YY1 and Bcl-xL expression in Ramos non-Hodgkin's lymphoma cell line via inhibition of NF- $\kappa$ B activity: role of YY1 and Bcl-xL in Fas resistance and chemoresistance, respectively. *J Immunol* 2005;175:2174-83.
13. Jazirehi AR, Bonavida B. Cellular and molecular signal transduction pathways modulated by rituximab (rituxan, anti-CD20 mAb) in non-Hodgkin's lymphoma: implications in chemosensitization and therapeutic intervention. *Oncogene* 2005;24:2121-43.
14. Daeron M. Building up the family of ITIM-bearing negative coreceptors. *Immunol Lett* 1996;54:73-6.
15. Fong DC, Brauweiler A, Minskoff SA, et al. Mutational analysis reveals multiple distinct sites within Fc  $\gamma$  receptor IIB that function in inhibitory signaling. *J Immunol* 2000;165:4453-62.
16. Nimmerjahn F, Ravetch JV. Fc $\gamma$  receptors: old friends and new family members. *Immunity* 2006;24:19-28.
17. Uray K, Medgyesi D, Hilbert A, Sarmay G, Gergely J, Hudecz F. Synthesis and receptor binding of IgG1 peptides derived from the IgG Fc region. *J Mol Recognit* 2004.
18. Wines BD, Powell MS, Parren PW, Barnes N, Hogarth PM. The IgG Fc contains distinct Fc receptor (FcR) binding sites: the leukocyte receptors Fc  $\gamma$  RI and Fc  $\gamma$  RIIa bind to a region in the Fc distinct from that recognized by neonatal FcR and protein A. *J Immunol* 2000;164:5313-531.
19. Armour KL, van de Winkel JG, Williamson LM, Clark MR. Differential binding to human Fc $\gamma$ RIIIa and Fc $\gamma$ RIIb receptors by human IgG wildtype and mutant antibodies. *Mol Immunol* 2003;40:585-93.
20. Zhu Z, Ghose T, Hoskin D, et al. Radioimmunotherapy of human B-cell chronic lymphocytic leukemia in nude mice. *Cancer Res* 1994;54:5111-5117.
21. Xiong D, Xu Y, Liu H, et al. Efficient inhibition of human B-cell lymphoma xenografts with an anti-CD20  $\times$  anti-CD3 bispecific diabody. *Cancer Lett* 2002;177:29-39.
22. Shan D, Ledbetter JA, Press OW. Signaling events involved in anti-CD20-induced apoptosis of malignant human B cells. *Cancer Immunol Immunother* 2000;48:673-683.
23. Kunzmann V, Ruediger T, Hallek M, Mueller-Hermelink HK, Wilhelm M. Tumor cell agglutination and not solely cytokine release as mechanism of adverse reactions during anti-CD20 monoclonal antibody (IDEC-C2B8, rituximab) treatment. *Blood* 2001;98:1991-2.
24. Jazirehi AR, Gan XH, De Vos S, Emmanouilides C, Bonavida B. Rituximab (anti-CD20) selectively modifies Bcl-xL and apoptosis protease activating factor-1 (Apaf-1) expression and sensitizes human non-Hodgkin's lymphoma B cell lines to paclitaxel-induced apoptosis. *Mol Cancer Ther* 2003;2:1183-93.
25. Alas S, Emmanouilides C, Bonavida B. Inhibition of interleukin 10 by rituximab results in down-regulation of bcl-2 and sensitization of B-cell non-Hodgkin's lymphoma to apoptosis. *Clin Cancer Res* 2001;7:709-23.
26. Wen WK, Levy R. Expression of complement inhibitors CD46, CD55, and CD59 on tumor cells does not predict clinical outcome after rituximab treatment in follicular non-Hodgkin lymphoma. *Blood* 2001;98:1352-7.
27. Farag SS, Flinn IW, Modali R, Lehman TA, Young D, Byrd JC. Fc  $\gamma$  RIIIIa and Fc  $\gamma$  RIIa polymorphisms do not predict response to rituximab

**Cancer Therapy: Preclinical**

- in B-cell chronic lymphocytic leukemia. *Blood* 2004;103:1472-4.
28. Canfield SM, Morrison SL. The binding affinity of human IgG for its high affinity Fc receptor is determined by multiple amino acids in the CH2 domain and is modulated by the hinge region. *J Exp Med* 1991;173:1483-91.
29. Thommesen JE, Michaelsen TE, Loset GA, Sandlie I, Brekke OH. Lysine 322 in the human IgG3 C(H)2 domain is crucial for antibody dependent complement activation. *Mol Immunol* 2000;37:995-1004.
30. Cardarelli PM, Quinn M, Buckman D, et al. Binding to CD20 by anti-B1 antibody or F(ab')<sub>2</sub> is sufficient for induction of apoptosis in B-cell lines. *Cancer Immunol Immunother* 2002;51:15-24.
31. Daeron M. Structural bases of Fcγ R functions. *Int Rev Immunol* 1997;16:1-27.
32. Pan L, Pei P. Signaling transduction by IgG receptors. *Chin Med J (Engl)* 2003;116:487-94.
33. O'Shea JJ, Weissman AM, Kennedy IC, Ortaldo JR. Engagement of the natural killer cell IgG Fc receptor results in tyrosine phosphorylation of the ζ chain. *Proc Natl Acad Sci U S A* 1991;88:350-4.
34. Galandrini R, Palmieri G, Piccoli M, Frati L, Santoni A. Role for the Rac1 exchange factor Vav in the signaling pathways leading to NK cell cytotoxicity. *J Immunol* 1999;162:3148-52.
35. Hazan-Halevy I, Seger R, Levy R. The requirement of both extracellular regulated kinase and p38 mitogen-activated protein kinase for stimulation of cytosolic phospholipase A(2) activity by either FcγRIIA or FcγRIIIB in human neutrophils. A possible role for Pyk2 but not for the Grb2-Sos-Shc complex. *J Biol Chem* 2000;275:12416-23.
36. Alas S, Ng CP, Bonavida B. Rituximab modifies the cisplatin-mitochondrial signaling pathway, resulting in apoptosis in cisplatin-resistant non-Hodgkin's lymphoma. *Clin Cancer Res* 2002;8:836-45.
37. Garban HJ, Bonavida B. Nitric oxide inhibits the transcription repressor Yin-Yang 1 binding activity at the silencer region of the Fas promoter: a pivotal role for nitric oxide in the up-regulation of Fas gene expression in human tumor cells. *J Immunol* 2001;167:75-81.

# Clinical Cancer Research

## Rituximab-Mediated Cell Signaling and Chemo/Immuno-sensitization of Drug-Resistant B-NHL Is Independent of Its Fc Functions

Mario I. Vega, Sara Huerta-Yepez, Melisa Martinez-Paniagua, et al.

*Clin Cancer Res* 2009;15:6582-6594. Published OnlineFirst November 2, 2009.

<b>Updated version</b>	Access the most recent version of this article at: doi: <a href="https://doi.org/10.1158/1078-0432.CCR-09-1234">10.1158/1078-0432.CCR-09-1234</a>
<b>Supplementary Material</b>	Access the most recent supplemental material at: <a href="http://clincancerres.aacrjournals.org/content/suppl/2009/10/27/1078-0432.CCR-09-1234.DC1">http://clincancerres.aacrjournals.org/content/suppl/2009/10/27/1078-0432.CCR-09-1234.DC1</a>

<b>Cited articles</b>	This article cites 36 articles, 21 of which you can access for free at: <a href="http://clincancerres.aacrjournals.org/content/15/21/6582.full#ref-list-1">http://clincancerres.aacrjournals.org/content/15/21/6582.full#ref-list-1</a>
-----------------------	--------------------------------------------------------------------------------------------------------------------------------------------------------------------------------------------------------------------------------------------

<b>Citing articles</b>	This article has been cited by 4 HighWire-hosted articles. Access the articles at: <a href="http://clincancerres.aacrjournals.org/content/15/21/6582.full#related-urls">http://clincancerres.aacrjournals.org/content/15/21/6582.full#related-urls</a>
------------------------	-----------------------------------------------------------------------------------------------------------------------------------------------------------------------------------------------------------------------------------------------------------

<b>E-mail alerts</b>	<a href="#">Sign up to receive free email-alerts</a> related to this article or journal.
----------------------	------------------------------------------------------------------------------------------

<b>Reprints and Subscriptions</b>	To order reprints of this article or to subscribe to the journal, contact the AACR Publications Department at <a href="mailto:pubs@aacr.org">pubs@aacr.org</a> .
-----------------------------------	------------------------------------------------------------------------------------------------------------------------------------------------------------------

<b>Permissions</b>	To request permission to re-use all or part of this article, use this link <a href="http://clincancerres.aacrjournals.org/content/15/21/6582">http://clincancerres.aacrjournals.org/content/15/21/6582</a> . Click on "Request Permissions" which will take you to the Copyright Clearance Center's (CCC) Rightslink site.
--------------------	----------------------------------------------------------------------------------------------------------------------------------------------------------------------------------------------------------------------------------------------------------------------------------------------------------------------------------